archives
of thermodynamics
Vol. **43**(2022), No. 2, 129–155
DOI: 10.24425/ather.2022.141982

Effect of serrated circular rings on heat transfer augmentation of circular tube heat exchanger

HIMANSHI KHARKWAL
SATYENDRA SINGH*

Department of Mechanical Engineering,
B.T. Kumaon Institute of Technology,
Dwarahat-263653 (Almora), Uttarakhand, India

Abstract Limiting energy resources has led researchers to find new innovative ways to enhance heat exchanging devices thermal performance in power generating systems. Thus, the present paper analyzes passive techniques of enhancing the thermal performance of a single tube heat exchanger. Experimental and numerical investigation on heat transfer enhancement using aserrated circular ring with twisted tape is carried out. The work incorporates the determination of Nusselt number, friction factor, thermal performance factor for serrated circular ring with twisted tape with variation in diameter ratio (0.8 and 0.85) and pitch ratio (2 and 3). Air is used as a working fluid with Reynolds number 6000–24000. The experiment is conducted by providing a constant wall heat flux of 1000 W/m^2 to the system and thereby taking results at a steady state. The experimental and computational findings obtained for the smooth tube case are compared with the standard correlations of Dittus–Boelter and Blasius. Based on experimental and numerical investigation, there is 5.16 times augmentation in heat transfer and 3.05 times improvement in thermal performance factor over the smooth tube heat exchanger. In addition, the study of entropy generation rate for every geometrical parameter has been conducted, and their influence on the system's thermal behaviour is presented. The results obtained in the present study may help the researchers of the same research area to find similar inserts and new ways of enhancing the thermal performance of heat exchangers.

Keywords: Heat transfer rate; Friction factor; Thermal performance factor; Serrated circular ring

*Corresponding Author. Email: ssinghiitd@gmail.com

Nomenclature

A	–	surface area of the pipe, m^2
A_o	–	area of orifice plate, m^2
C_d	–	coefficient of discharge
c_p	–	specific heat of the air, $Jkg^{-1}K^{-1}$
D	–	test section diameter, m
d	–	inner diameter of circular insert, m
DR	–	diameter ratio, = d/D
D_h	–	hydraulic diameter, m
f	–	friction factor
f_s	–	friction factor for smooth tube
g	–	gravitational acceleration, m s^{-2}
h	–	average convective heat transfer coefficient, $Wm^{-2}K^{-1}$
k	–	thermal conductivity of air, $Wm^{-1}K^{-1}$
l	–	distance between two consecutive inserts, m
L	–	test section length, m
PR	–	pitch ratio, = l/D
m	–	air flow rate, kg s^{-1}
N_S	–	entropy generation number
Nu	–	Nusselt number
Nu_s	–	Nusselt number for smooth tube
Pr	–	Prandtl number
ΔP	–	pressure difference, Pa
ΔP_O	–	pressure difference across orifice plate, Pa
$\dot{Q}_{\text{air}}$	–	heat carried by air, W
$\dot{Q}_{\text{conv}}$	–	heat transfer by convection, W
$\dot{Q}_{VI}$	–	heat input, W
Re	–	Reynolds number
S_g	–	entropy generation rate, kW K^{-1}
$S_{g,r}$	–	entropy generation rate for rough tube, kW K^{-1}
$S_{g,s}$	–	entropy generation rate for smooth tube, kW K^{-1}
T	–	temperature, K
T_{fm}	–	fluid mean temperature, K
T_i	–	inlet air temperature, K
T_o	–	outlet air temperature, K
T_{wm}	–	wall mean temperature, K
TPF	–	thermal performance factor
t	–	time, s
v	–	velocity of air ms^{-1}
TR	–	twist ratio, = y/w

Greek symbols

μ	–	dynamic viscosity of fluid, Pa s
ρ	–	density, kg m^{-3}

Subscripts

fm	–	fluid mean value
o	–	exit
O	–	orifice
p	–	pipe

Abbreviations

CFD	–	computational fluid dynamics
SCR	–	serrated circular ring
SCRTT	–	serrated circular ring with twisted tape
UHF	–	uniform heat flux

1 Introduction

Safe and reliable operations demand highly effective heat exchanger, either in electronic microdevices or bulky mechanical component like boiler. Among the several modes of heat transfer, convective heat transfer is the most efficient one. However few years' back traditional methods of heat transfer were practiced, *viz.* natural and forced convection. But in this new era of modern science, advanced technologies for enhancing the heat transfer phenomena are being studied by researchers. The heat transfer enhancement could be done either by providing pulsating cams, fluid vibrations, reciprocating plungers or by placing secondary surfaces like inserts, fins. Providing an external power source is known as an active technique, whereas the application of secondary surfaces is referred to as a passive technique of heat transfer augmentation.

When placed in the tube of heat exchanger, secondary surfaces or the inserts alter the heat transfer rate and pressure drop in that area. Previously studied inserts by researchers are twisted tapes, tubes, rings, and many more. Numerical and experimental investigation on dimpled rib heat exchanger was done by Kumar *et al.* [1] and cross ellipsoidal dimples were studied numerically by Xie *et al.* [2], in which it was found that dimple depth, pitch and axis ratio play an important role in heat transfer process. Tube [3], cylindrical blade tube [4], small pipe [5], spirally corrugated tube [6], vortex rod [7] when used in the heat exchanger's tube, showed an increment in heat transfer rate. Converging-diverging tubes along with twin counter swirling twisted tape was used by Yuziang *et al.* [8] and it was noticed that all set of different geometrical parameters have performance greater than 1. Another type of inserts used for heat transfer en-

hancement is the delta winglets [9]. For best results wings should be in forward direction [10] and it was also noticed that as the number of delta wings and its attack angle increases heat transfer and pressure losses also increases [11, 12].

Singh *et al.* [13] studied the effect of circular and elliptical insert with vertical twisted tape and got thermal performance factor (TPF) of 2.43. Multiple inserts when studied by Vashistha *et al.* [14] revealed that 4 counter swirl twisted tape provides an enhancement of 1.26 in TPF. In tube twisted tape design was used by Alzaharani and Usman *et al.* [15]. In their investigation they varied the width and twist ratio of twisted tape and got maximum augmentation of 28% in heat transfer rate. Double counter twisted tape when used by Bhuyia *et al.* [16] gave performance enhancement of 1.34 for twist ratio of 1.95. Further Suri *et al.* [17] square perforated the twisted tape and found that perforated ones have better enhancement in heat transfer as compared to non-perforated and plane tube. Twisted tape with double V-cut and other cut shapes was done by Nakhchi and Esfahani [18, 19]. They reported that double V-cut insert has a better enhancement of 1.83 whereas single cut twisted tape has enhancement of 1.64 compared to that of smooth tube. Hong *et al.* [20] used multiple twisted tapes along with sinusoidal rib tube whereas Bas and Ozceyhan [21] placed the twisted tape separately from tube wall. Similarly, study of twisted tape with varying cut edges was done by Sarviya and Fuskele [22] in which they concluded that continuous rectangular cut twisted tapes are much more beneficial than the plain tube.

Computational fluid dynamics (CFD) analysis of helically coiled tube heat exchanger was done by Reddy *et al.* [23] and their investigation revealed that addition of semi-circular baffles increases heat transfer coefficient by 10%. While Keklikcioglu and Ozceyhan [24] in their experimental investigation showed equilateral triangle cross-sectional coiled wire inserts gives performance intensification of 1.67. Gholamalizadeh *et al.* [25] in their investigation studied the heat transfer intensification phenomenon using coiled wire inserts. Some modifications on helical coil were done by other researchers like perforated discontinuous helix turbulators was used by Sheikholeslami *et al.* [26] and coil with different arrangements was studied by Eiamsa-ard *et al.* [27].

Surface disturbances in fluid flow using solid hollow circular ring was done by Kongkaitpaiboon *et al.* [28] while perforation on circular rings was done by Kumar *et al.* [29] and it was noticed that perforated circular rings have better augmentation than the solid circular rings. Whereas

Singh *et al.* [30] in their experimental investigation used rectangular wings along with the circular rings and got a TPF of 1.95. Further Pandey and Singh [31] used triangular perforated Y-shape inserts in their studies, gives maximum heat transfer and TPF. Hollow cross disk was studied by Zong *et al.* [32]. They reported hollow cross disks have approximately twice larger performance enhancement than the twisted tapes of width ratio 2.5:1. Circular ring-metal wire net [33] inserts when used in circular heat exchanger gave TPF of 2.84 for pitch ratio of 3. Nakhchi and Esfahani in their numerical investigation studied the effect of different geometrical parameters on perforated conical rings in which effect of conical ring diameter ratio and hole diameter ratio was studied [34]. Table 1 shows previous experimental and numerical investigation on heat exchanger tube having different inserts.

Table 1: Previous investigation on heat exchanger tube with different inserts.

Shape type	Geometry	Nature of work	Conditions	Principle findings
Dimpled rib [1]		Numerical and experimental	• $4000 \leq \text{Re} \leq 28000$ • Variation in stream wise spacing, span wise spacing, ratio of dimpled depth to print diameter	$\text{Nu}/\text{Nu}_s = 3.18$ TPF = 2.87
Cross ellipsoidal dimples [2]	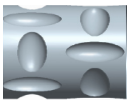	Numerical	• $5000 \leq \text{Re} \leq 30000$ • Variation in dimples depth, pitch and axis ratio	TPF = 1.58 at depth = 2 mm, pitch = 20 mm, axis ratio = 2.2 and Re = 5000.
Double-sided Delta-wing [10]	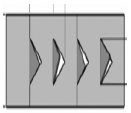	Experimental	• $4000 < \text{Re} < 20000$ • Variation in arrangement, axis, wing-width ratios and wing-pitch ratios	$\text{Nu}/\text{Nu}_s = 165\%$ $f/f_s = 14.8$ TPF=1.19
Double counter twisted tape [16]	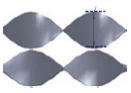	Experimental	• $6950 \leq \text{Re} \leq 50050$ • Variation in twist ratios of: 1.95, 3.85, 5.92, 7.75	$\text{Nu}/\text{Nu}_s = 60 - 240\%$, $f/f_s = 91 - 286\%$ TPF= 1.34 with double counter twisted tapes

Continued on next page

Table 1 [cont.]

Shape type	Geometry	Nature of work	Conditions	Principle findings
Twisted tape [21]		Experimental	• $5132 \leq \text{Re} \leq 24989$ • Variation in twist ratios of: 2, 2.5, 3, 3.5, 4 and clearance ratios of: 0.0178, 0.0357	TPF = 1.756 for clearance ratio of 0.0178 and twist ratios of 2 at Re = 5183.
Twisted tape with continuous cut edges [22]	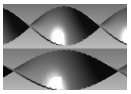	Experimental	• $4000 < \text{Re} < 20000$. • Variation in twist ratios of 3, 5	Nu/Nu_s for twist ratios5 and 3 are 2.21–1.85 and 2.23–1.89 f/f_s for twist ratios 5 and 3 are 2.9 and 3.5 times while TPF for twist ratios 5 and 3 falls in the ranges of 1.31–1.56, 1.26–1.46, respectively
Circular-ring [28]	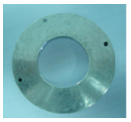	Experimental	• $4000 \leq \text{Re} \leq 20000$. • Variation in diameter ratios of 0.5, 0.6 and 0.7 and pitch ratios $= 6, 8$ and 12	$\text{Nu}/\text{Nu}_s = 57 - 195\%$
Circular perforated ring [29]		Experimental	• $6500 \leq \text{Re} \leq 23000$ • Variation in diameter ratios of: 0.6, 0.7, pitch ratio of 1 and perforation index of 8%, 16%, 24%	Nu/Nu_s augments about 4 times in case of perforation index of 8% and diameter ratios of 0.6 while TPF augments 1.47 times in case of perforation index of 24% and diameter ratios of 0.8
Metal wire net inserts [33]		Experimental	• $5000 \leq \text{Re} \leq 40000$ • Variation in wire net grades of 4, 9, 16, and pitch ratio of 2, 3, 4	Nu/Nu_s augments around 3.35 times over the smooth tube case for pitch ratio of 2, and wire net grade of 16,while maximum TPF = 2.84 at pitch ratio of 3, and wire net grade of 9
Delta-wing tape inserts [36]	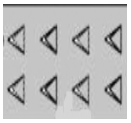	Experimental and numerical	• $4200 \leq \text{Re} \leq 25500$ • Variation in wing inclination angles of 30°, 45°, 60° and ratios of wing-pitch to tube-diameter of 0.5, 1.0, 1.5, 2.0, 2.5	$\text{Nu}/\text{Nu}_s = 505\%$ $f/f_s = 69$ TPF = 1.49

Some other inserts examined by researchers are: Aerofoil shaped [35], delta wing tape [36], ellipse and super ellipse based corrugated tube [37], baffles [38], triangular copper fin with twisted tape [39], right-left helical with spacer [40], inclined vortex rings [41], hexagonal conical rings [42], center tapered wavy type [43], curved winglets [44], louvered strip [45], rectangular winglets with circular punched holes [46], ribbed and corrugated surfaces [52], staggered V shape obstacles [53].

From the above literature it is obtained that, various types of inserts *viz.* circular insert, twisted tapes, delta wings, etc. has been used by researchers. However, there are more possibilities of heat transfer enhancement by techniques possessing both core and surface disturbances. Also, the growing need to serve various manufacturing difficulties shows a provision for carrying this present study. On the other hand, literature studied shows that number of twisted tapes affects the performance i.e., for better performance of heat exchanger, both the parameters *viz.* heat transfer rate and friction factor should be optimum. Thus, the number of twisted tapes selected was one. In this paper serrated circular rings with twisted tape is investigated experimentally and computationally. The effect of diameter ratio and pitch ratio serrated circular ring is tested for Reynolds number ranging from 6000–24000. The results obtained include Nusselt number, friction factor and thermal performance factor.

2 Experimental work

2.1 Material and experimental model setup

The experimental set up is fabricated as per the literature survey. The schematic representation of experimental set up is shown in Fig. 1.

Heat exchanger is made from a galvanized iron tube of $D_h = 68$ mm. It comprises mainly 3 sections: inlet section, outlet section, and test section. For ensuring the fully developed hydrodynamic flow, inlet section is made 2700 mm long. While the length of the test section is 1500m and it has essential components like a variant transformer, thermocouples, voltmeter, ammeter, and digital manometer. No heat loss to the surrounding by the system has been assured by using glass wool fibre and insulated pads as insulation in the test section. For evaluating temperature difference 24 T-type thermocouples have been used. These thermocouples are calibrated with a thermostat, before being used for the investigation. The deviation noted while calibration ranges within ± 0.3°C. The thermocouples in the experimental set up are distributed as follows: 1 in inlet section, 20 in test

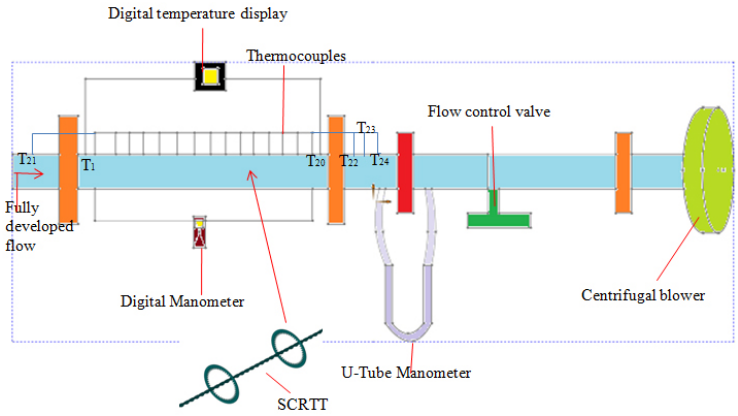

Figure 1: Schematic representation of experimental setup.

section, and 3 in outlet section. Average wall temperature is calculated by finding the arithmetic mean of local temperature measured by each thermocouple. Therefore, 20 thermocouples were decided to be used in the test section, neglecting the minor deviations. The net temperature value is calculated by finding the mean value of local temperatures provided at the 1st to 20th position. A thermocouple at the 21st position is used to check the air temperature at the inlet section. Similarly, three thermocouples were employed at the outlet section. The net outlet temperature is calculated by taking the mean value of thermocouples placed at the 22nd, 23rd, and 24th positions. Also, to ensure proper temperature estimation, these thermocouples were placed uniformly but at 90° radial distance. Thus the temperature distribution throughout the surface area could be measured.

Furthermore, these thermocouples are connected to the digital temperature display, where the output of each can be noted down. The pressure difference prevailing in the test section has been calculated using a digital manometer. The outlet section is made 1500 mm long and possesses the flow controlling and measuring devices like: flow control valve, orifice meter, U-tube manometer, and 2238 W blower.

2.2 Range of parameters

Serrated circular ring is a modification of circular rings [29]. It possesses an inner circle having diameter d and an outer circle having diameter D. Ratio of these two diameters is known as diameter ratio. Serrations in the ring are made from the inner circle and point towards the center of the ring. Heat exchanger with serrated circular ring with twisted tape (SCRTT) was

tested for optimum conditions. The dimensionless parameters which define SCRTT are: diameter ratio, pitch ratio, and twist ratio. A variation made in these parameters is listed in Table 2. The schematic and photographic diagram of SCRTT is shown in Figs. 2 and 3.

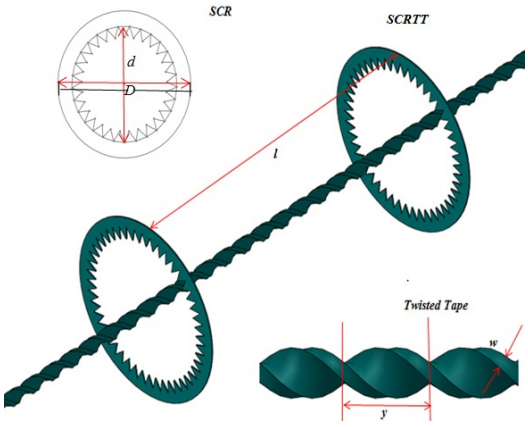

Figure 2: Schematic representation of serrated circular ring with twisted tape.

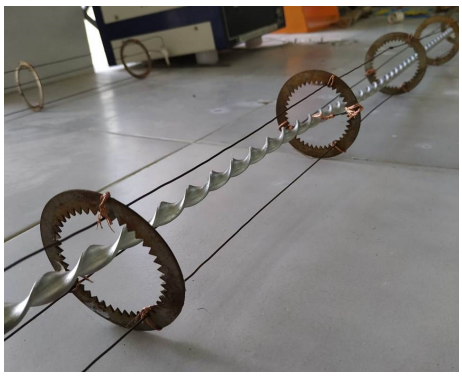

Figure 3: The serrated circular ring with twisted tape with diameter ratio of 0.8 and pitch ratio of 3.

Table 2: Range of parameters.

Parameter	Range
Diameter ratio	0.8, 0.85
Pitch ratio	2, 3
Twist ratio	4 (fixed)
Reynolds number	6000–24000

2.3 Research methodology and measurement techniques

The experimental set up shown in Fig. 4 has been used for experimental investigation. Initially the experimental setup was tested and validated with the standard empirical correlations of Dittus-Boelter and Blasius for smooth tube case. Following the validation, the Nusselt number (Nu) and friction factor (f) were calculated for heat exchanger having SCRTT. The following procedure has been adopted for conducting experimentation: Air is used as the working medium. The velocity of air is varied using a flow control valve. The working fluid passes the long inlet chamber for ensuring the formation of a fully developed flow. Following it, air enters in the premises of the test section which possess serrated circular rings along with a twisted tape. In the test section, the wall of the heat exchanger pipe is being heated by a nichrome wire heater connected with a variant transformer allowing a uniform heat flux (UHF) of 1000 Wm^{-2} to the system. As working fluid moves forward along the length of the tube, due to temperature difference its tiny particles take up the heat prevailing in the system, and thus forced convection is said to occur in the heat exchanger. This heated air after travelling the whole distance moves towards the outlet section and gets emerged in the environment through the blower opening. The parameters of interest in this whole process are the average convective heat transfer coefficient (h) and pressure difference (ΔP). As stable conditions persist, data required for the calculation is withdrawn.

Figure 4: Pictorial representation of experimental setup.

The experimental investigation is carried for Reynolds number (Re) ranging from 6000–24000. To ensure whether steady-state has been reached, a heat calibration test has been performed between the coil winding and the heat absorbed by the air. The test revealed that, for each experimental

run, the variation in heat supplied by coil winding and the heat gained by air lies between $5-7\%$:

$$\left|\left(\frac{\dot{Q}_{VI}-\dot{Q}_{\text{air}}}{\dot{Q}_{VI}}\right)\right| < (5-7)\,\%. \tag{1}$$

Considering only forced convection, it is assumed that the heat gained by air is equal to the heat lost in convection. Therefore, it can be written as

$$\dot{Q}_{\text{air}} = \dot{Q}_{\text{conv}}\,, \tag{2}$$

The heat gained, $\dot{Q}_{\text{air}}$, and lost, $\dot{Q}_{\text{conv}}$, are calculated as

$$\dot{Q}_{\text{air}} = mc_p\,(T_o - T_i)\,, \tag{3}$$

$$\dot{Q}_{\text{conv}} = hA\,(T_{wm} - T_{fm})\,, \tag{4}$$

where m is the air flow rate, c_p is the specific heat of the air, A is the surface area of the pipe, T_{wm}, T_i, and T_0 are the average values given by the thermocouples:

$$\begin{aligned} T_{wm} &= \frac{(T_1+T_2+\ldots+T_{20})}{20}\,, \quad T_i = T_{21}, \quad \text{and} \\ T_0 &= \frac{(T_{22}+T_{23}+T_{24})}{3}\,, \end{aligned} \tag{5}$$

while T_{fm} is the average of inlet and outlet temperature

$$T_{fm} = \frac{(T_i+T_o)}{2}\,. \tag{6}$$

Orifice plate in the test section assembled with U-tube manometer gives the value of mass flow rate through which flow velocity is calculated. Further, Reynolds number is evaluated using formula

$$\text{Re} = \frac{\rho v D}{\mu}\,, \tag{7}$$

where D is the diameter of test section, ρ and μ are the density and dynamic viscosity of the fluid.

The important parameters in this study are h, f and Nu which are calculated as:

$$h = \frac{mc_p\,(T_o - T_i)}{A\,(T_{wm} - T_{fm})}\,, \tag{8}$$

$$f = \frac{\Delta P}{\left(\frac{L}{D}\right)\left(\frac{\rho V^2}{2}\right)}, \tag{9}$$

$$\mathrm{Nu} = \frac{hD}{k}, \tag{10}$$

where k is the thermal conductivity of air and L is the test section length.

The thermal performance of the heat exchanger is evaluated using a factor given by Webb and Kim [47], which is

$$\mathrm{TPF} = \frac{(\mathrm{Nu}/\mathrm{Nu}_s)}{(f/f_s)^{1/3}}. \tag{11}$$

Here Nu_s and f_s are calculated using the empirical correlations of Dittus–Boelter and Blasius, which are:

$$\text{Dittus–Boelter Correlation} \qquad \mathrm{Nu}_s = 0.023\mathrm{Re}^{0.8}\mathrm{Pr}^{0.4}, \tag{12}$$

$$\text{Blasius Correlation} \qquad f_s = 0.316\mathrm{Re}^{-0.25}. \tag{13}$$

Entropy generation rate (S_g) and entropy generation number, (N_s) are calculated using the correlation given by Keklikcioglu and Ozceyhan [50]:

$$S_g = \frac{q^2}{\pi T_{fm}^2 k\mathrm{Nu}} + \frac{32m^3 f}{\pi^2 \rho^2 T_{fm} D^5}, \tag{14}$$

$$N_s = \frac{S_{g_r}}{S_{g_s}}, \tag{15}$$

where q defines the wall heat transfer rate per meter length of tube.

2.4 Uncertainty analysis and validation of experimental results

2.4.1 Uncertainty analysis

Error associated with experimental instruments was estimated with the criteria given by Kline and McClintock [48].The uncertainty analysis was carried out for single case geometry in whole selected range of Re. Uncertainty in results for non-dimensional parameters are calculated using equations provided below:

uncertainty in mass flow rate:

$$\Delta m = \left[\left(\frac{\partial m}{\partial C_d}\Delta C_d\right)^2 + \left(\frac{\partial m}{\partial \rho_O}\Delta \rho_O\right)^2 + \left(\frac{\partial m}{\partial A_O}\Delta A_O\right)^2 + \left(\frac{\partial m}{\partial (\Delta P)_o}\Delta(\Delta P)_o\right)^2\right]^{0.5}, \tag{16}$$

uncertainty in heat gain:

$$\frac{\Delta Q}{Q} = \left[\left(\frac{\Delta m}{m}\right)^2 + \left(\frac{\Delta c_p}{c_p}\right)^2 + \left(\frac{\Delta(\Delta T)}{\Delta T}\right)^2\right]^{0.5}, \tag{17}$$

uncertainty in heat transfer coefficient:

$$\frac{\Delta h}{h} = \left[\left(\frac{\Delta Q_u}{Q_u}\right)^2 + \left(\frac{\Delta A_p}{A_p}\right)^2 + \left(\frac{\Delta\left(\Delta T_{fm}\right)}{\Delta T_{fm}}\right)^2\right]^{0.5}, \tag{18}$$

uncertainty in Reynolds number:

$$\frac{\Delta \mathrm{Re}}{\mathrm{Re}} = \left[\left(\frac{\Delta D}{D}\right)^2 + \left(\frac{\Delta V}{V}\right)^2 + \left(\frac{\Delta \rho}{\rho}\right)^2 + \left(\frac{\Delta \mu}{\mu}\right)^2\right]^{0.5}, \tag{19}$$

uncertainty in Nusselt Number:

$$\frac{\Delta \mathrm{Nu}}{\mathrm{Nu}} = \left[\left(\frac{\Delta D}{D}\right)^2 + \left(\frac{\Delta h}{h}\right)^2 + \left(\frac{\Delta k}{\Delta k}\right)^2\right]^{0.5}, \tag{20}$$

uncertainty in friction factor:

$$\frac{\Delta f}{f} = \left[\left(\frac{\Delta D}{D}\right)^2 + \left(\frac{\Delta L}{L}\right)^2 + \left(\frac{\Delta \rho}{\rho}\right)^2 + \left(\frac{\Delta V}{V}\right)^2 + \left(\frac{\Delta(\Delta P)}{\Delta P}\right)^2\right]^{0.5}. \tag{21}$$

The error calculation results are listed in Table 3.

Table 3: Range of uncertainty for different parameters.

Parameter	Range (%)
Mass flow rate	2.93
Heat gain	3.12
Heat transfer coefficient	3.19
Reynolds number	2.73
Nusselt number	2.53
Friction factor	6.57

2.4.2 Validation of experimental results

A comparative study has been conducted to validate the experimental results of present work. In this study, experimental results of smooth tube case were compared with the empirical correlations of Dittus–Boelter and Blasius. Further these results were compared with the prior work of Kumar *et al.* [49].The comparative study showed that the average deviations in results are ±3.11, ±3.19 for Nu and f respectively. Validation of experimental results is shown in Fig. 5.

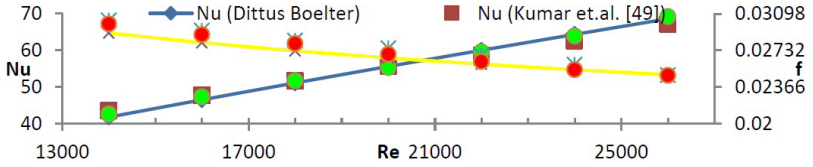

Figure 5: Comparison of present work with standard correlations and Kumar *et al.* [49].

3 Computational work

3.1 Computational investigation and boundary conditions

Computational investigation on evaluating the thermal performance of heat exchanger using SCRTT is performed using commercial finite element analysis software Ansys fluent [54]. For doing the numerical simulation, initially geometry and physical properties i.e., bounds are to be defined. Therefore, fluid domain is made in the "geometry" cell of simulation software and the necessary boundary conditions are applied directly to the fluid domain. Fluid domain consists of a circular tube having diameter 68.1 mm and length 1500 m. Converting a governing equation into an algebraic equation is known as discretization. Grid elements are obtained by discretization of geometry into non-overlapping discrete elements. This process is known as meshing. The discretization of the physical domain produces a computational mesh on which the governing equations are solved. Also, a solution is said to converge when it does not change further as the iterations proceed. The finite volume method possesses much flexibility since discretization is carried directly in the physical space, and there is no requirement of any transformation between the physical system and the computational coordinate system. Therefore, discretization method adopted here is finite volume method with a convergence criterion of 10^{-6}.

SIMPLE algorithms are used for pressure velocity coupling [55]. It solves the flow problem iteratively by generating a velocity and pressure field that satisfies the continuity and momentum equations while approaching the final solution at every iteration.The geometrical and computational conditions used in the analysis are shown in Tables 4 and 5.

Table 4: Geometrical conditions considered in computational simulation.

Geometrical parameters	
Geometry	SCRTT
DR	0.8, 0.85
PR	2, 3
TR	4

Table 5: Computational and boundary conditions considered in computational simulation.

Computational conditions	
Dimensional	3-dimensional
Method	finite volume
Turbulence model	standard $k-\varepsilon$
Fluid	Air ($\rho = 1.225$ kg/m^3, $\mu = 1.7894 \times 10^{-5}$, $c_p = 1006.43$ J/kgK)
Inlet temperature	300 K
Reynolds number	6000−24000
Wall condition	constant wall heat flux (1000 W/m^2)
Flow condition	periodic flow
Hydraulic diameter	0.0681 m
Boundary conditions	
Velocity inlet	$v = 0$, $w = 0$, Re = 6000−24000, $T_{\text{in}} = 300$ K
Pressure outlet	$P = P_{\text{atm}}$
Wall	$Q = 1000$ W/m^2
Material	aluminium

3.2 Governing equations

Continuity, momentum and energy equations [56] are used for analysing the conditions of flowing fluid in the heat exchanger. Continuity equation is given by

$$\frac{\partial}{\partial x_i}(\rho u_i) = 0. \tag{22}$$

Momentum equation is given by

$$\frac{\partial \vec{V}}{\partial t} + \vec{V} \cdot \nabla \vec{V} = \frac{1}{\rho}\left(-\nabla P + \mu \nabla^2 \vec{V} + \rho \beta \vec{g}\,(T - T_0) + \vec{S}\right). \tag{23}$$

Energy equation is given by

$$\frac{\partial H}{\partial t} + \nabla \cdot \left(\vec{V} H\right) = \nabla \left(\frac{k}{\rho c_p} \nabla h\right). \tag{24}$$

3.3 Mesh sensitivity analysis

For checking the variation in computational results grid independence test has been conducted as shown in Table 6. Grid independence test is a process to find the optimum grid conditions with the smallest number of grids without generating any variation in results with respect to grid conditions. The CFD model used for grid independence contains a tube of length 1500 m and diameter 68mm and serrated circular rings with diameter ratio 0.8 and pitch ratio 2. Grid elements are varied by altering relevance center and smoothing. Further, the effect of increasing grid elements on the convergence rate is observed. It can be noted from the table that the deviation in Nu and f is minimum in the case of meshing having fine relevance center and high smoothing. But at the same time, it possesses a large number of mesh elements which will take a lot of time for solving process. Therefore, meshing with 18, 30, and 180 elements were selected such that the deviation in results would be smaller with comparatively less computational time. The same procedure has been adopted for the rest of the geometries. Meshing of fluid domain is shownin Fig. 6.

Table 6: Grid independence test for serrated circular ring DR = 0.8 and PR = 2.

Relevance centre	Smoothing	Elements	Nodes	Nu	$\left\lvert\frac{\mathrm{Nu}^{i+1} - \mathrm{Nu}^{i}}{\mathrm{Nu}^{i}}\right\rvert$	f	$\left\lvert\frac{f^{i+1} - f^{i}}{f^{i}}\right\rvert$
Coarse	Low	658066	736626	176.67	–	2.1354	–
Coarse	Medium	658130	736623	180.87	0.0238	2.2218	0.0405
Medium	Medium	1830070	2052222	185.45	0.0253	2.3522	0.0587
Medium	High	1830180	2052222	187.84	0.0129	2.4254	0.0311
Fine	Low	263926	2984017	188.27	0.0023	2.4321	0.0028
Fine	Medium	2639643	2984017	188.53	0.0014	2.4347	0.0011
Fine	High	2639886	2984017	188.64	0.0006	2.4352	0.0002

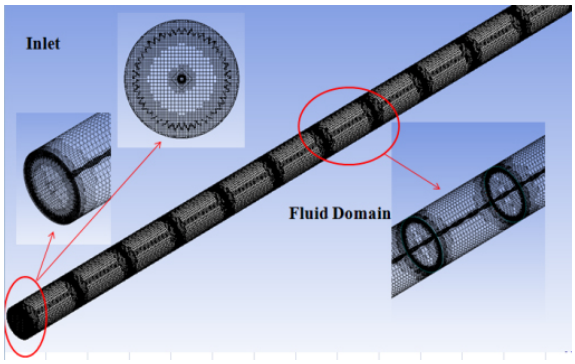

Figure 6: Meshing in SCRTT.

4 Results and discussion

In this type of heat exchanger, forced convection exists. When the air particles come in contact with heated tube walls, they absorb heat from the tube which in result increases their kinetic energy and molecular momentum. Hence particles near vicinity of tube become less dense and due to buoyancy effects less dense particles rises and denser particle sinks. This repeated phenomenon gives rise to convection currents. The main parameters on which convection depends are area and temperature difference. Along with these parameters, efficiency of heat exchanger can be enhanced by producing some artificial obstructions in the path of fluid flow. Due to these obstructions strong swirls are generated near tube walls which give rise to flow disturbances. These disturbances in return give rise to diffusion. Thus, rate of convection increases.

In the present study, the intensity of disturbance generated is studied using three parameters *viz.* PR, DR, and Re. These parameters directly affect swirls generation which in return alters friction factor too. Thus TPF of heat exchanger varies.

4.1 Computational simulations

Computational simulation was carried out on all the 6 geometrical parameters. It shows that the frequent attachments and detachments of fluid streamlines intensify the fluid mixing process, which enhances convection process inside the tube. Hindrance generated near SCRTT is shown with the help of vector representation in Fig. 7.

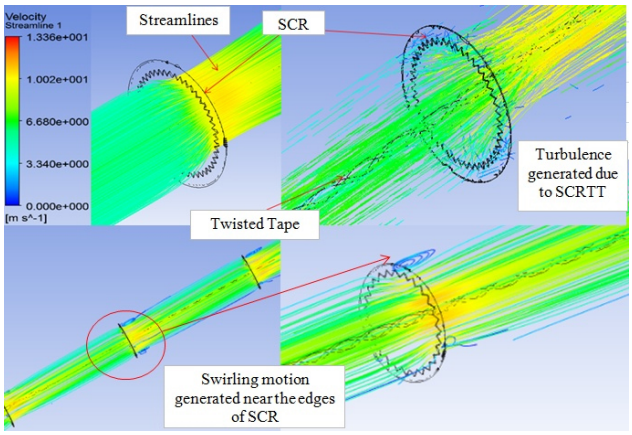

Figure 7: Turbulence generated inside the tube due to SCRTT.

4.2 Effect on Nusselt number

The serrated circular ring with twisted tape was tested for Re ranging from 6000–24000. Effect of SCRTT on the Nusselt number is shown in Fig. 8. As we alter the geometrical and flow parameters Nu varies accordingly. In this study the two geometrical parameters considered were: pitch ratio and diameter ratio. When PR ratio increases the distance between consecutive inserts also increases. Due to which intensity of turbulence decreases and hence it decreases heat transfer also. Thus, lower values of PR gives better heat transfer rate. The reason for getting such trend is the decrement in the

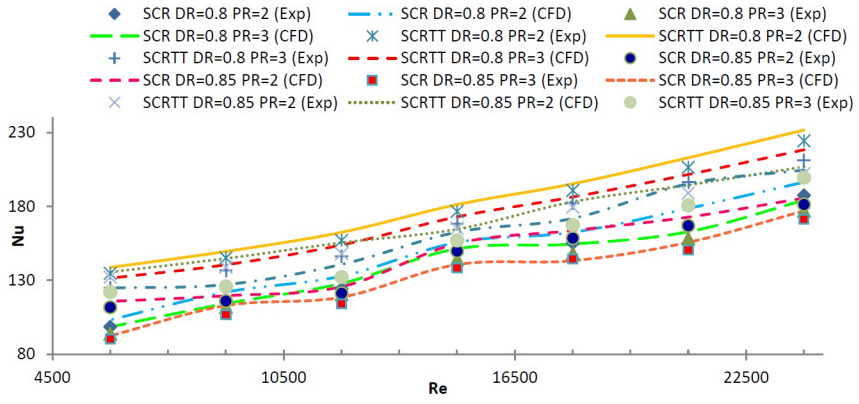

Figure 8: Variation in Nu with Re.

laminar sublayer. The laminar sublayer acts as a resistance to heat transfer between surface and heat transfer fluid. The existence of inserts decreases the thickness of laminar sublayer in thermal boundary layer and therefore, the resistance to convective heat transfer decreases and heat transfer increases between surface and heat transfer fluid.

The flow parameter considered in this study is Reynolds number. It can be noticed in the figure that increasing Re results in enhancing Nu. This happens because increasing Re gives higher turbulence which leads to enhancement in Nu. With increase in DR the heat transfer rate decreases because the surface contact of fluid decreases which results in lesser hindrance and thus lesser intermixing. Ratio of heat transfer rate in circular tube having SCRTT with respect to smooth tube is known as the enhancement ratio for heat transfer rate. The enhancement ratio Nu/Nu_s *versus* Re is plotted in Fig. 9.

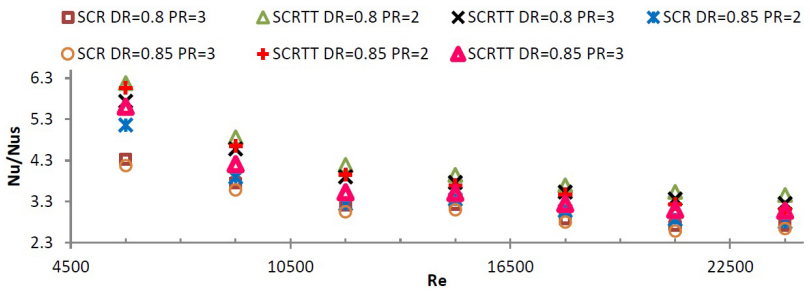

Figure 9: Variation in Nu/Nu_s with Re.

4.3 Effect on friction factor

Performance of a heat exchanger depends not only in heat transfer rate, but also in the friction persisting inside the tube. Cases where surface contact of fluid is larger, suffers larger friction. Because it intensifies the collision process that moves air particles in a vigorous way. These air particles when collide with each other increases the pressure difference and also intensify the frictional energy inside the tube. Similar thing happens in present case too, when air particles strike with SCR, pressure difference increases which give rise to frictional energy. Effect of SCRTT on friction factor is shown in Fig. 10.

Due to higher surface contact area and lesser distance among inserts, SCRTT having DR = 0.8 and PR = 2 exhibits higher friction factor. This is because the two factors; higher surface contact area and lesser distance.

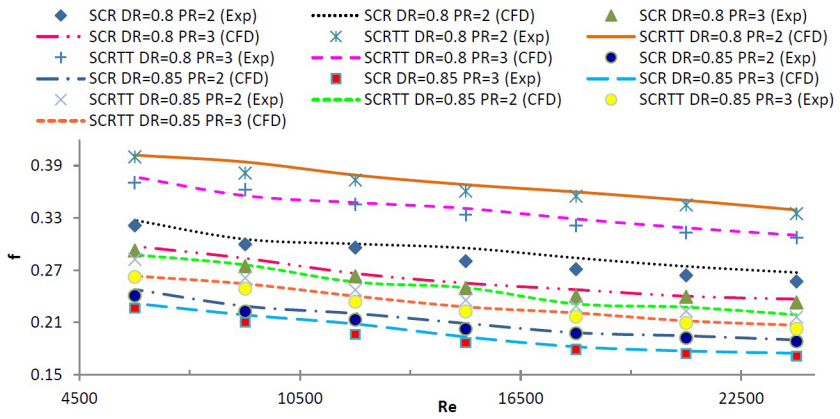

Figure 10: Variation in friction factor with Re.

These two leads to higher turbulence inside the test section. Particles colliding with each other in a very vibrant way resist flow, which increases friction inside the tube. Effect of SCRTT on f/f_s is shown in Fig. 11. It can be noticed from the figure that as velocity increases the enhancement ratio for friction increases.

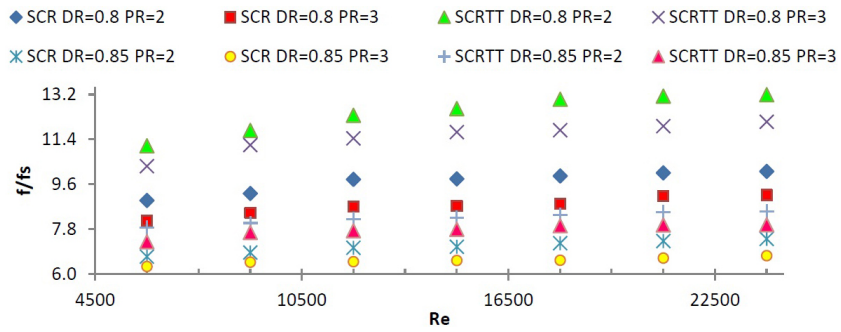

Figure 11: Variation in f/f_s with Re.

4.4 Effect on thermal performance factor

Thermal performance factor is a function of Nusselt number and friction factor. For a heat exchanger system, to have maximum efficiency $\mathrm{Nu}/\mathrm{Nu}_s$ should be larger and f/f_s should be smaller. Therefore we have to select a case having optimum values of these two parameters. Variation in TPF with Re is shown in Fig. 12. It can be noticed, that maximum TPF occurs

at Re = 6000. The maximum TPF obtained is 3.05 for SCRTT having DR = 0.85 and PR = 2.

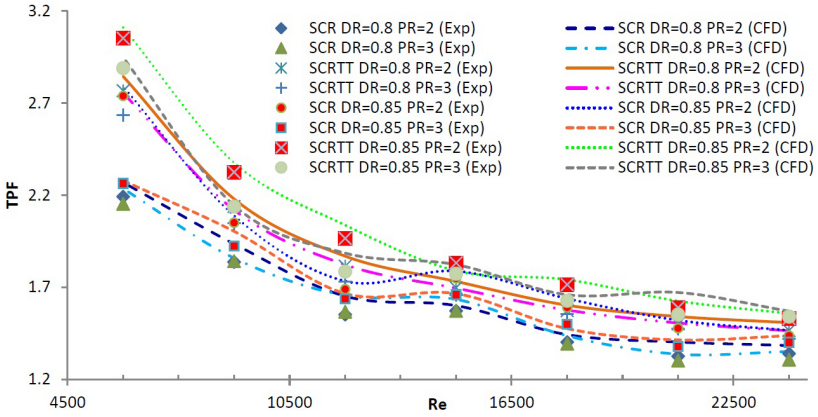

Figure 12: Variation in TPF with Re.

4.5 Entropy generation number

The increased turbulence inside the heat exchanger tube enhances the random motion of particles and thus generates irreversibility in the flow, which gives rise to entropy generation. A thermodynamic system is said to be advantageous when entropy generation number (Ns) is lower than unity.

Variation of entropy generation number for different geometrical parameters of SCRTT has been plotted in Fig. 13. It can be seen in the figure that

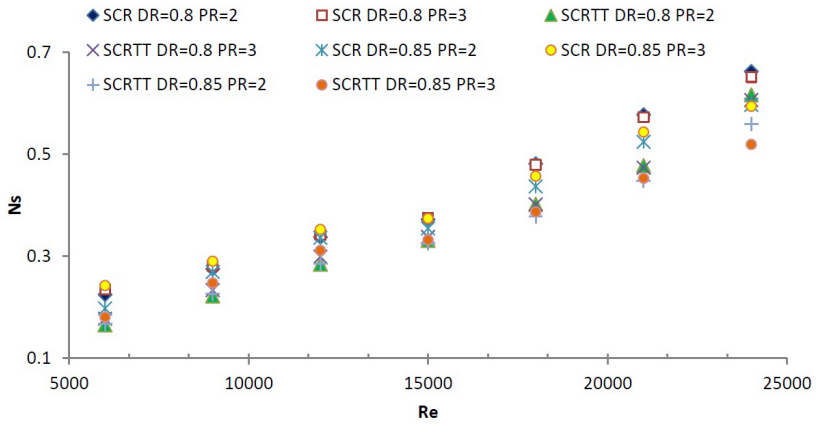

Figure 13: Entropy Generation plot for different geometrical parameters of SCRTT.

with increase in Re, Ns increases. This is due to the increase in randomness. For better results, geometries with least entropy generation number should be selected. Therefore, SCRTT with DR = 0.8 and PR = 2 is considered when Re < 15000 and SCRTT with DR = 0.85 and PR = 3 is considered when Re > 15000.

5 Comparison with previous work

The present work has been compared with some inserts used previously by researchers which were having same range of Re. The inserts are: double V-cut twisted tape inserts [18], aerofoil shaped [35], inclined vortex rings [41], hexagonal conical rings [42], curved winglet tapes [44], and louvered strip [45]. It can be seen in Fig. 14 that SCRTT with DR = 0.85 and PR = 2 exhibits highest TPF among these inserts.

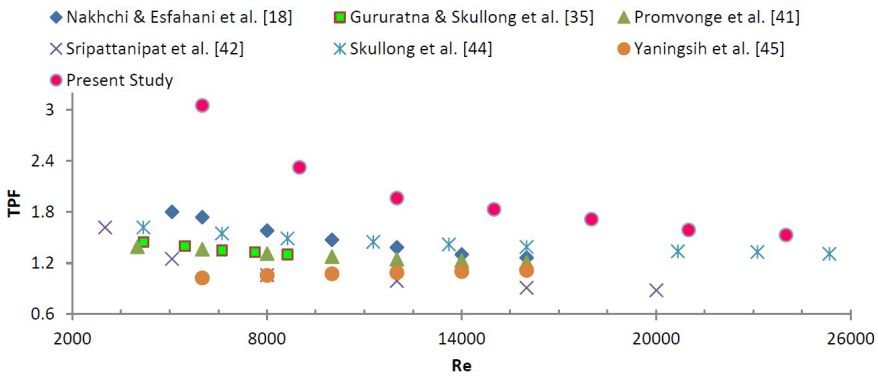

Figure 14: Comparison of SCRTT with some previously used inserts of researchers.

Furthermore, comparative analysis of present study has been done with previous work of Singh *et al.* [13,51]. The inserts selected from our previous studies are elliptical rings, circular ring with vertical twisted tape (CVTT), elliptical ring with vertical twisted tape (EVTT) and perforated curved circular rings (PCCR). The comparative analysis shown in Fig. 15 revealed that the TPF of SCRTT is higher than inserts like CVTT, EVTT, elliptical rings, PCCR.

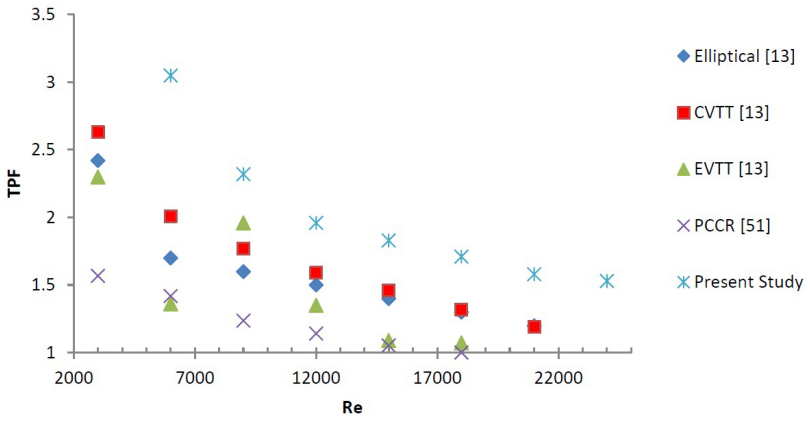

Figure 15: Comparison of SCRTT with previous work of Singh *et al.* [13, 51].

6 Conclusions

The heat transfer, friction factor, and thermal performance characteristics of a single tube heat exchanger with SCRTT have been examined experimentally and computationally. Serrated circular rings with diameter ratio (0.8, 0.85) and pitch ratio (3, 4) have been used for investigation. Eight cases with different diameter ratios and pitch ratios are performed. It is found from the research that serrated circular ring with diameter ratio 0.85 and pitch ratio 2 gives thermal performance factor of 3.05 at Reynolds number of 6000, where Nusselt number and friction factor are 5.16 and 6.19 times above the smooth tube. In addition, a study on entropy generation has been performed, which revealed that for Reynolds number less than 15000, SCRTT with diameter ratio 0.8 pitch ratio 2 and for Reynolds number greater than 15000 SCRTT with diameter ratio 0.85 and pitch ratio 3 gives a lower value of entropy generation number. Thus, it makes them a better choice for the respective range of Reynolds number. Comparative results of SCRTT with other inserts like elliptical rings, circular rings with vertical twisted tape, elliptical rings with vertical twisted tape, and perforated curved circular rings are also determined.

Furthermore, energy-saving in thermodynamic systems is crucial to coping with the limiting energy sources issue. Therefore, practices should be adopted to make heat exchanging devices more effective. One such method of increasing the heat transfer capacity of a single tube heat exchanger has been discussed in the present article. Similarly, investigation for SCRTT

with nano fluid can be performed, and their effect on heat transfer characteristics can be studied.

Received 31 October 2021

References

[1] Kumar A., Maithani R., Suri A.: *Numerical and experimental investigation of enhancement of heat transfer in dimpled rib heat exchanger tube*. Heat Mass Transfer **53**(2017), 3501–3516.

[2] Xie S., Liang Z., Zhang L., Wang Y.: *A numerical study on heat transfer enhancement and flow structure in enhanced tube with cross ellipsoidal dimples*. Int. J. Heat Mass Tran. **125**(2018), 434–444.

[3] Abu-Khader M.: *Further understanding of twisted tape effects as tube insert for heat transfer enhancement*. Heat Mass Transfer **43**(2006), 123–134.

[4] Karagoz S., Afshari F., Yildirim O., Comakli O.: *Experimental and numerical investigation of the cylindrical blade tube inserts effect on the heat transfer enhancement in the horizontal pipe exchangers*. Heat Mass Transfer **53**(2017), 2769–2784.

[5] Tu W., Tang Y., Hu J., Wang Q., Lu L.: *Heat transfer and friction characteristics of laminar flow through a circular tube with small pipe inserts*. Int. J. Therm. Sci. **96**(2015), 94–101.

[6] Xin F., Liu Z., Zheng N., Liu P., Liu W.: *Numerical study on flow characteristics and heat transfer enhancement of oscillatory flow in a spirally corrugated tube*. Int. J. Heat Mass Tran. **127**(2018), 402–413.

[7] Zheng N., Liu P., Wang X., Shan F., Liu Z., Liu W.: *Numerical simulation and optimization of heat transfer enhancement in a heat exchanger tube fitted with vortex rod inserts*. Appl. Therm. Eng. **123**(2017), 471–484.

[8] Yuxiang H., Xianhe D., Lianshan Z.: *3Dnumerical study on compound heat transfer enhancement of converging-diverging tubes equipped with twin twisted tapes*. Chinese J. Chem. Eng. **20**(2012), 589–601.

[9] Akcayoglu A.: *Flow past confined delta-wing type vortex generators*. Exp. Therm. Fluid Sci. **35**(2011), 112–120.

[10] Eiamsa-ard S., Promvonge P.: *Influence of double-sided delta-wing tape insert with alternate-axes on flow and heat transfer characteristics in a heat exchanger tube, fluid flow and transport phenomena*. Chinese J. Chem. Eng. **19**(2011), 410-423.

[11] Khoshvaght-Aliabadi M., Sartipzadeh O., Alizadeh A.: *An experimental study on vortex-generator insert with different arrangements of delta-winglets*. Energy **82**(2015), 629–639.

[12] Promvonge P., Khanoknaiyakarn C., Kwankaomeng S., Thianpong C.: *Thermal behavior in solar air heater channel fitted with combined rib and delta-winglet*. Int. Commun. Heat Mass Tran. **38**(2011), 749–756.

[13] Singh S., Pandey L., Kharkwal H., Sah H.: *Augmentation of thermal performance of heat exchanger using elliptical and circular insert with vertical twisted tape.* Exp. Heat Transfer 33 (2019), 6, 510–525.

[14] Vashishtha C., Patil A., Kumar M.: *Experimental investigation of heat transfer and pressure drop in a circular tube with multiple inserts.* Appl. Therm. Eng. **96**(2016), 117–129.

[15] Alzahrani S., Usman S.: *CFD simulations of the effect of in-tube twisted tape design on heat transfer and pressure drop in natural circulation.* Therm. Sci. Eng. Prog. **11**(2019), 325–333.

[16] Bhuiya M.M.K., Sayema A.S.M., Islam M, Chowdhury M.S.U., Shahabuddin M.: *Performance assessment in a heat exchanger tube fitted with double counter twisted tape inserts.* Int. Commun. Heat Mass Tran. **50**(2014), 25–33.

[17] Suri A., Kumar A., Maithani R.: *Heat transfer enhancement of heat exchanger tube with multiple square perforated twisted tape inserts.* Exp. Invest. Corr. Dev. **116**(2017) 76–96.

[18] Nakhchi M.E., Esfahani J.A.: *Performance intensification of turbulent flow through heat exchanger tube using double V-cut twisted tape inserts.* Chem. Eng. Process. Process Intensific. **141**(2019), 107533.

[19] Nakhchi M.E., Esfahani J.A.: *Numerical investigation of rectangular-cut twisted tape insert on performance improvement of heat exchangers.* Int. J. Therm. Sci. **138**(2019), 75–83.

[20] Hong Y., Du J., Li Q., Xu T., Li W.: *Thermal-hydraulic performances in multiple twisted tapes inserted sinusoidal rib tube heat exchangers for exhaust gas heat recovery applications.* Energ. Convers. Manage. **185**(2019), 271–290.

[21] Bas H., Ozceyhan V.: *Heat transfer enhancement in a tube with twisted tape inserts placed separately from the tube wall.* Exp. Therm. Fluid Sci. **41**(2012), 51–58.

[22] Sarviya R.M., Fuskele V.: *Heat transfer and pressure drop in a circular tube fitted with twisted tape insert having continuous cut edges.* J. Energ. Stor. **19**(2018), 10–14.

[23] Reddy V., Kumar S., Gugulothu R., Anuja K., Rao V.: *CFD analysis of a helically coiled tube in tube heat exchanger.* Sci. Direct Mater. Today Proc. **4**(2017), 2341–2349.

[24] Keklikcioglu O., Ozceyhan V.: *Experimental investigation on heat transfer enhancement in a circular tube with equilateral triangle cross sectional coiled wire insert.* Appl. Therm. Eng. **131**(2018), 686–695.

[25] Gholamalizadeh E., Hosseini E., Jamanani M., Amiri A., Sare A., Alimoradi A.: *Study of intensification of the heat transfer in helically coiled tube heat exchanger via coiled wire inserts.* Int. J. Therm. Sci. **141**(2019), 72–83.

[26] Sheikholeslami M., Gorji-Bandpy M., Ganji D.: *Effect of discontinuous helical turbulators on heat transfer characteristics of double pipe water to air heat exchanger.* Energ. Convers. Manage **118**(2016), 75–87.

[27] Eiamsa-ard S., Nivesrangsan P., Chokphoemphun S., Promvonge P.: *Influence of combined non-uniform wire coil and twisted tape inserts on thermal performance characteristics.* Int. Commun. Heat Mass Tran. **37**(2010), 850–856.

[28] Kongkaitpaiboon V., Nanan K., Eiamsa-ard S.: *Experimental investigation of convective heat transfer and pressure loss in a round tube fitted with circular-ring turbulators*. Int. Commun. Heat Mass Tran. **37**(2010), 568–574.

[29] Kumar A., Chamoli S., Kumar M., Singh S.: *Experimental investigation on thermal performance and fluid flow characteristics in circular cylindrical tube with circular perforated ring inserts*. Exp. Therm. Fluid Sci. **79**(2016), 168–174.

[30] Singh S., Negi J., Bisht S., Sah H.: *Thermal performance and frictional losses study of solid hollow circular disc with rectangular wings in circular tube*. Heat Mass Tran. 55(2019), 2975–2986.

[31] Pandey L., Singh S.: *Numerical analysis for heat transfer augmentation in circular tube heat exchanger using triangular perforated Y-shape insert*. Fluids **6**(2021), 7, 247.

[32] Zong Y., Bai D., Zhou M., Zhao L.: *Numerical studies on heat transfer enhancement by hollow-cross disk for cracking coils*. Chem. Eng. Process. Process Intensific. **135**(2019), 82–92.

[33] Bartwal A., Gautam A., Kumar M., Mamgrulkar C., Chamoli S.: *Thermal performance intensification of a circular heat exchanger tube integrated with compound circular ring-metal wire net inserts*. Chem. Eng. Process. Process Intensific. **124**(2018), 50–70.

[34] Nakchi M.E, Esfahani J.A.: *Numerical investigation of different geometrical parameters of perforated conical rings on flow structure and heat transfer in heat exchanger*. Appl. Therm. Eng. **156**(2019), 494–505.

[35] Gururatana S., Skullong S.: *Experimental investigation of heat transfer in a tube heat exchanger with airfoil-shaped insert*. Case Stud. Therm. Eng. **14**(2019).

[36] Skullong S., Promvonge P., Jayranaiwachira N., Thianpong C.: *Experimental and numerical heat transfer investigation in a tubular heat exchanger with delta-wing tape inserts*. Chem. Eng. Process. **109**(2016), 164–177.

[37] Navickaite K., Cattani L., Bahl C., Engelbrecht K.: *Elliptical double corrugated tubes for enhanced heat transfer*. Int. J. Heat Mass Tran. **128**(2019) 363–377.

[38] Andrzejczyk R., Muszynski T., Gosz M.: *Experimental investigations on heat transfer enhancement in shell coil heat exchanger with variable baffles geometry*. Chem. Eng. Process. **132**(2018), 114–126.

[39] Hameed V., Hussein M.: *Effect of new type of enhancement on inside and outside surface of the tube side in single pass heat Exchanger*. Appl. Therm. Eng. **122**(2017), 484–491.

[40] Nagarajan P.K., Sivashanmugam P.: *Heat transfer enhancement studies in a circular tube fitted with right-left helical inserts with spacer*. World Ac. Sci., Eng. Technol., Int. J. Mech. Mechatron. Eng. **5**(2011), 10, 2091–2095.

[41] Promvonge P., Koolnapadol N., Pimsarn M., Thianpong C.: *Thermal performance enhancement in a heat exchanger tube fitted with inclined vortex rings*. Appl. Therm. Eng. **62**(2014), 285–292.

[42] Sripattanapipat S., Tamna S., Jayranaiwachira N., Promvonge P.: *Numerical heat transfer investigation in a heat exchanger tube with hexagonal conical-ring inserts*. Energy Proced. **100**(2016), 522–525.

[43] Liang Y., Liu P., Zheng N., Shan F., Liu Z., Liu W.: *Numerical investigation of heat transfer and flow characteristics of laminar flow in a tube with center-tapered wavy-tape insert*. Appl. Therm. Eng. **148**(2019), 557–567.

[44] Skullong S., Promvonge P., Thianpong C., Jayranaiwachira N., Pimsarn M.: *Thermal performance of heat exchanger tube inserted with curved-winglet tapes*. Appl. Therm. Eng. **129**(2018), 1197–1211.

[45] Yaningsih I., Wijayanta A., Miyazaki T., Koyama S.: *Thermal hydraulic characteristics of turbulent single-phase flow in an enhanced tube using louvered strip insert with various slant angles*. Int. J. Therm. Sci. **134**(2018), 355–362.

[46] Modi A., Kalel N., Rathod M.: *Thermal performance augmentation of fin-and-tube heat exchanger using rectangular winglet vortex generators having circular punched holes*. Int. J. Heat Mass Tran. **158**(2020), 119724.

[47] Webb R.L., Kim N.H.: *Principles of Enhanced Heat Transfer* (2nd Edn.). Taylor Francis, New York 2005.

[48] Klein S.J., McClintock A.: *The description of uncertainties in a single sample experiments*. Mech. Eng. **75**(1953), 3–8.

[49] Kumar A., Chamoli S., Kumar M.: *Experimental investigation on thermal performance and fluid flow characteristics in heat exchanger tube with solid hollow circular disk inserts*. Appl. Therm. Eng. **100**(2016), 227–236.

[50] Keklikcioglu O., Ozceyhan V.: *Entropy generation analysis for a circular tube with equilateral triangle cross sectioned coiled-wire inserts*. Energy **139**(2017), 65–75.

[51] Singh S., Kharkwal H., Gautam A., Pandey A.: *CFD analysis for thermo-hydraulic properties in a tubular heat exchanger using curved circular rings*. J. Therm. Anal. Calorim. **141**(2020), 2211–2218.

[52] Siddique W., Raheem A., Aqeel M., Qayyum S., Salamen T., Waheed K., Qureshi K.: *Evaluation of thermal performance factor for solar airheaters with artificially roughened channels*. Arch. Mech. Eng. **68**(2021), 195–225.

[53] Menni Y., Chamkha A., Zidani C., Benyoucef B.: *Analysis of thermo-hydraulic performanceof a solar air heater tube with modern obstacles*. Arch. Thermodyn. **41**(2020), 3, 33–56.

[54] https://www.ansys.com/products/fluids/ansys-fluent

[55] https://idoc.pub/queue/ansys-fluent-users-guide-d49o6jd0g649

[56] Benlekkam M., Nehar D.: *Hybrid nano improved phase change material for latent thermal energy storage system: Numerical study*. Arch. Mech. Eng. **69**(2022), 77–98.